ASYMPTOTICALLY-CORRECT STRUCTURAL MODELLING OF THIN-WALLED ANISOTROPIC CLOSED CROSS-SECTION ROTATING SLENDER BEAMS

F. Khouli, F.F. Afagh and R.G. Langlois
Department of Mechanical and Aerospace Engineering,
Carleton University, Ottawa, Ontario, Canada
E-mail: fafagh@mae.carleton.ca

Abstract

An application of a comprehensive and compact methodology to obtain the asymptotically-correct stiffness matrix of anisotropic, thin-walled, closed cross-section, and rotating slender beams is presented. The Variational Asymptotic Method (VAM), which utilizes small geometrical parameters inherent to thin-walled slender beams, is used to obtain the displacement and strain fields, and the cross-sectional stiffness matrix without any ad hoc assumptions. The advantage of this approach is that the asymptotically-correct and populated 4×4 cross-sectional stiffness matrix provides all the necessary information about the elastic behavior of the rotating beam, thereby nullifying the need for refined beam theories that incorporate higher order deformation modes, like the Vlasov's mode. The implementation of the theory using MATLAB was validated against the Vartiational Asymptotic Beam Sectional Analysis (VABS) computer software, a two-dimensional finite element program that utilizes a more general approach to the VAM that is applicable to thick/thin-walled anisotropic cross-sections with arbitrary geometry. Sample applications of the theory to rotor blades are presented. The paper concludes with a discussion of how the presented material would be used directly in the dynamic modelling of rotating helicopter blades.

Introduction

The structural dynamics modelling of rotating composite blades closely follows the advances made in capturing the elastic behavior of anisotropic, slender, and rotating beams with arbitrary cross-sectional geometry. In the past, the highly coupled structural and dynamics aspects of the model along with its strong nonlinearity proved to be an unyielding obstacle, and engineers were forced to adopt various approximations that limited the scope and applications of their models (Volovoi et al., 2001), and were later proved to be less than stellar in predicting the behavior of the rotating blades (Hodges and Patil, 2005, Volovoi et al., 2001). Some modifications were added to these models, which improved their performance, but not to the levels required for today's advances in composite and highly flexible blades. However, these modified preliminary models are still used by the industry today despite existing limitations. One may attribute this to be the result of their simplicity in terms of their formulation, and the experience and insight into their functioning that has been accumulated over time. Performing 3D finite element analysis on the rotating composite blades is an expensive and an unfeasible option even with current computational capabilities, especially when the analysis is directed at devising vibration control strategies or studying the structural dynamics interaction of the blades with other rigid/flexible multibody systems.

Recent advances in the cross-sectional modelling of anisotropic composite beams with arbitrary geometry is a major triumph in overcoming the difficulties discussed above. It was found that for slender beams, asymptotical analysis of the 3D elastic energy can split the problem into a two-dimensional analysis over the cross-section and one-dimensional analysis along the span of the

M. Pandey et al. (eds), Advances in Engineering Structures, Mechanics & Construction, 537–547.

beam without any ad hoc assumptions. Utilizing other geometrical design aspects of the rotor blade, one can also arrive at a closed form solution of the stiffness properties of the cross-section. This significantly reduces the amount of effort the engineer has to spend on modelling the elastic behavior of the blade, since the asymptotically-correct development is found to be surprisingly compact for a problem that seemed to be impossibly complex from the earlier models' point of view.

The VAM was originally developed by Berdichevsky (1982) for elastic slender rods that have an inherent small dimensionless parameter, which is the slenderness ratio defined by the ratio of the characteristic dimension of the cross-section, 'a', to the elastic deformation wavelength, 'l'. Since only global elastic deformation modes that propagate along most of the beam span are of interest here, the deformation length is always of the order of the length of the beam. The theory was refined by Hodges and Cesnik (1994) and implemented in Variational Beam Sectional Analysis (VABS), a software package that utilizes the finite element method to obtain the elastic constants of any composite cross-sections with initial twist. VABS has been extensively validated against experimental data and results from other reliable 3D finite element software like ABAQUS and NASTRAN (Yu et al., 2002). Concurrently, Badir (in Berdichevsky et al., 1992) expanded the theory to thin-walled composite beams that have an additional small dimensionless parameter, which is the thinness ratio defined by the ratio of the thickness of the wall, 'h', to the characteristic dimension of the cross-section, 'a'. This allowed for a simple closed form solution for the stiffness constants, which has been used to model rotor blades with active materials (Cesnik and Shin, 1998, 2001a, 2001b). However, it was later found that Badir's work neglected the shell bending strain measure, which made it asymptotically-incorrect and produced results inconsistent with those produced by VABS for certain cross-sections. Hodges and Volovoi (2000) identified and corrected this flaw, and developed the asymptotically-correct theory for anisotropic thin-wall beams.

Rotor blades can be idealized as thin-walled closed cross-section beams while retaining high degree of fidelity. The asymptotically-correct theory has been successfully implemented using MATLAB to arrive at the elastic properties of any closed cross-section including helicopter rotor blades, which are at the centre of many research efforts of the Applied Dynamics Group at Carleton University. The versatility of the implementation allows it to obtain the elastic properties about any desired point in the plane of the cross-section like the elastic axis of the blade. Additionally, it allows for any desired material composition and distribution throughout the cross-section.

Theory

The Variational Asymptotic Method

A brief symbolic outline of the VAM and its general features is presented to complement the subsequent discussion. Let the 3D elastic energy of the beam be symbolically defined by the energy functional $\mathcal{F}$ with the small parameter that is for now called η such that (Cesnik, 1994):

$$\begin{aligned} \mathcal{F}(\Gamma, \eta) &= \mathcal{E}_1(\Upsilon, z_1) + \mathcal{E}_{\eta 0}(\Upsilon, z_1, \eta), \\ z_1 &= \begin{bmatrix} w_{11} & w_{12} & w_{13} \end{bmatrix}, \end{aligned} \tag{1}$$

where Γ is a 6×1 column matrix that represents the 3×3 symmetric Biot–Jaumann strain field, and Υ is a function of the axial coordinate along the span of the beam only (in this case it corresponds to Γ) (Danielson and Hodges, 1987).

The energy functional $\mathcal{F}$ is decomposed into two parts: $\mathcal{E}_1(\Upsilon, z_1)$ which contains all terms of order $\eta^0 \equiv 1$ and $\mathcal{E}_{\eta 0}(\Upsilon, z_1, \eta)$ that contain all terms of order η^1 and higher with respect to this small parameter. The vector z_1 represents a perturbation in the classical 3D displacement field, which in reality is the in/out-of-plane warping functions to a first correction, that gives rise to low and high

order terms as is apparent from its appearance in both parts of the energy functional. In order to find the first correction to the displacement field, z_1, the high-order component of the functional is discarded and then the functional is minimized with respect to z_1. The solution of the Euler minimization problem is not unique and the displacement field is four times redundant. The four rigid body modes have to be eliminated from z_1 (the warping field) over the surface area of the cross-section S, therefore, the following four constraints are imposed:

$$\begin{aligned} \min_{z_1} \mathcal{F} &= \min_{z_1} \mathcal{E}_1(\Upsilon, z_1), \\ \int_S \mathcal{C}_1(z_1)\, \mathrm{d}s = 0, \quad \int_S \mathcal{C}_2(z_1)\, \mathrm{d}s &= 0, \quad \int_S \mathcal{C}_3(z_1)\, \mathrm{d}s = 0, \quad \int_S \mathcal{C}_4(z_1)\, \mathrm{d}s = 0. \end{aligned} \tag{2}$$

When Equations (2) are solved over the cross-section they yield what is called the "zeroth-approximation" or the building block of the solution, z_1. This must not be confused with the order of the components of z_1 itself, which could be of some order of η, but rather it refers to it being obtained by minimizing the part of the energy that has zeroth order of η (i.e., η^0). In most cases, there is no closed form solution for z_1, and the problem is discretized over the cross-section with the constraints leading to a Sturm–Liouville problem followed by finite element calculations, which is the methodology of VABS (Cesnik et al., 1993, Cesnik and Hodges, 1997). The order of the components of z_1 is not known a priori but determined throughout the minimization procedure. The solution of Euler equations of the functional is symbolically written as:

$$z_1 = f_1(\Upsilon, \zeta_2, \zeta_3), \tag{3}$$

where ζ_2 and ζ_3 are the perpendicular axes defining the 2D Cartesian plane of the cross-section.

The displacement field is then perturbed again. Let the new perturbation be called z_2 such that:

$$z_2 = z_1 - f_1(\Upsilon, \zeta_2, \zeta_3). \tag{4}$$

The new perturbation is substituted back into the energy functional of Equation (1) to obtain:

$$\begin{aligned} \mathcal{F}(\Gamma, \eta) &= \mathcal{F}_1(\Upsilon) + \mathcal{E}_2(\Upsilon, z_2) + \mathcal{E}_{\eta 1}(\Upsilon, z_2, \eta), \\ z_2 &= \begin{bmatrix} w_{21} & w_{22} & w_{23} \end{bmatrix}. \end{aligned} \tag{5}$$

The function $\mathcal{F}_1(\Upsilon)$ represents all the terms that do not contain the new unknown, z_2. It is subscripted with 1 to indicate that it contains contributions from the first correction to the displacement field z_1. The function $\mathcal{E}_2$ contains the lowest-order terms involving z_2, while $\mathcal{E}_{\eta 1}$ contains all high-order terms.

Following the same procedure as before, the high order terms (i.e., $\mathcal{E}_{\eta 1}$) are discarded and the functional is minimized with respect to z_2 subject to the same constraints:

$$\begin{aligned} \min_{z_2} \mathcal{F} &= \mathcal{F}_1(\Upsilon) + min_{z_2} \mathcal{E}_2(\Upsilon, z_2) \\ \int_S \mathcal{C}_1(z_2)\, \mathrm{d}s = 0, \quad \int_S \mathcal{C}_2(z_2)\, \mathrm{d}s &= 0, \quad \int_S \mathcal{C}_3(z_2)\, \mathrm{d}s = 0, \quad \int_S \mathcal{C}_4(z_2)\, \mathrm{d}s = 0. \end{aligned} \tag{6}$$

Similarly,

$$z_2 = f_2(\Upsilon, \zeta_2, \zeta_3). \tag{7}$$

The process is repeated until the new perturbation yields no terms in the energy functional of order that is of the highest yielded by the previous perturbation, and at this point the displacement field is said to have converged. For example, assume that the perturbation z_k produced terms in the energy

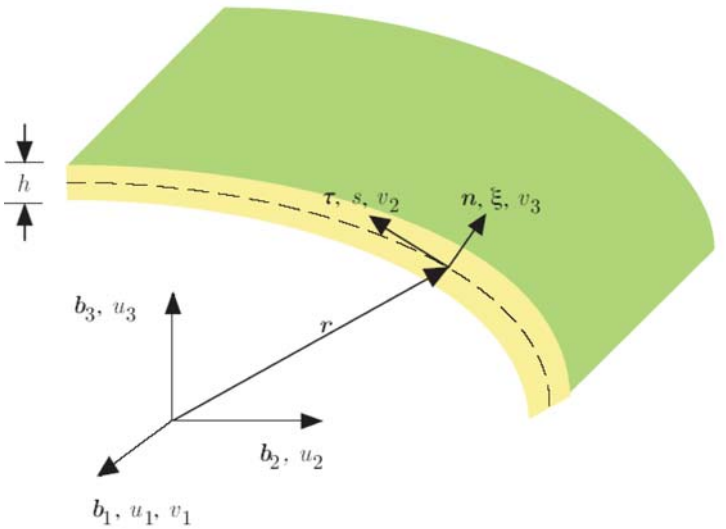

Fig. 1. Shell/thin-walled bar coordinate systems (Hodges and Volovoi, 2000).

functional with one being the highest order having an order of $\mathcal{O}(n)$. A further perturbation, z_{k+1}, produces terms that are of order $\mathcal{O}(n+1)$ and higher, then at this stage the iteration is terminated. In fact, one may not have to go as far as this in order to obtain the correct elastic behavior of the beam since η is a small parameter to start with. Terms of order $\mathcal{O}(\eta^0 \equiv 1)$ are the only ones needed to obtain the asymptotically-correct global elastic behavior of the beam.

The energy functional can then be written after the kth perturbation as:

$$\mathcal{F}(\Gamma,\eta) = \mathcal{F}_1(\Upsilon) + \mathcal{F}_2(\Upsilon) + \cdots + \mathcal{F}_k(\Upsilon) + \mathcal{E}_{k+1}(\Upsilon, z_{k+1}, \eta) + \mathcal{E}_{\eta k}(\Upsilon, z_{k+1}, \eta). \tag{8}$$

Alternatively, the energy functional can be expanded implicitly as an asymptotic series in the small parameter η:

$$\mathcal{F}(\Gamma,\eta) = \mathcal{O}(\eta^0) + \mathcal{O}(\eta^1) + \mathcal{O}(\eta^2) + \mathcal{O}(\eta^3) + \cdots + \mathcal{O}(\eta^k). \tag{9}$$

It must be evident by now that no ad hoc assumptions are made in order to arrive at the asymptotically-correct stiffness matrix that can be extracted from terms of order $\mathcal{O}(\eta^0)$. The process of dropping high order terms during the minimization or truncating them from the asymptotic expansion of the functional is equivalent to a correct and systematic neglect of insignificant terms in more conventional solution methods that rely on the Theory of Elasticity, equilibrium equations, and boundary conditions. But these conventional methods usually involve a multitude of partial differential equations, rendering the identification of these insignificant terms extremely difficult if not outright impossible.

The Asymptotically-Correct Stiffness Matrix

Hodges and Volovoi (2000, 2002) applied the VAM to thin-wall open/closed shells and strips depicted in Figure 1, and obtained the asymptotically-correct stiffness matrix for each case respectively. The intersection of the middle surface of the shell with the plane of the beam cross-section defines the contour s, which does not change along the span of the beam.

The energy functional of the composite beam in this case is the elastic shell energy per unit area written in terms of the six generalized shell strain measures:

$$\begin{aligned} 2\mathcal{U}_{\text{shell}} &= \psi^T Q\psi + 2\phi^T S\psi + \phi^T P\phi \\ \psi^T &= \left[\begin{array}{ccc} \gamma_{11} & h\rho_{11} & h\rho_{12} \end{array}\right] \\ \phi^T &= \left[\begin{array}{ccc} 2\gamma_{12} & \gamma_{22} & h\rho_{22} \end{array}\right], \end{aligned} \tag{10}$$

where Q, S, and P are material property matrices that depend on the 2D elastic modulus tensor of the material, which is obtained from the reduced stiffness coefficients Q_{mn} of Classical Laminate Theory (Badir, 1992).

The six generalized shell strain measures are given in terms of the curvilinear displacements, which in turn can be expressed in terms of the cartesian displacements u_1, u_2, and u_3:

$$\begin{array}{ll} \gamma_{11} = v_{1,1} & \rho_{11} = v_{3,11}, \\ 2\gamma_{12} = v_{1,2} + v_{2,1} & \rho_{12} = v_{3,12} + \frac{1}{4R}(v_{1,2} - 3v_{2,1}), \\ \gamma_{22} = v_{2,2} + \frac{v_3}{R} & \rho_{22} = v_{3,22} - (\frac{v_2}{R})_{,2}, \end{array} \tag{11}$$

The subscripted comma indicates a differentiation with respect to the curvilinear coordinate subsequent to it, and R is the radius of curvature defined using the cartesian coordinates x_2 and x_3 along b_2 and b_3 respectively as $R = \dot{x}_2/\ddot{x}_3 = -\dot{x}_3/\ddot{x}_2$. The over-dot implies a differentiation with respect to the curvilinear coordinate s. The generalized strain measures in Equation (11) are substituted in the shell energy in Equation (10) and integrated over the contour to give the functional:

$$\oint 2\mathcal{U}_{\text{shell}}\, \mathrm{d}s \equiv \mathcal{F}(\psi, \phi). \tag{12}$$

It is reemphasized in this problem, that two small dimensionless parameters are present: the slenderness ratio $\eta_1 = a/l$, and the thinness ratio $\eta_2 = h/a$. All deformation modes are assumed to have the same order of magnitude $\mathcal{O}(\epsilon)$, and therefore they are all included in the development to make it general: extension, torsion, bending about the b_2 axis, and bending about the b_3 axis.

An asymptotic expansion of the shell energy functional in terms of the small parameters is sought in the form:

$$\begin{aligned} \oint 2\mathcal{U}_{\text{shell}} &= \mathcal{O}(\epsilon^2 \cdot \eta_1^0 \cdot \eta_2^0) + \mathcal{O}(\epsilon^2 \cdot \eta_1^1 \cdot \eta_2^0) + \\ &\quad + \mathcal{O}(\epsilon^2 \cdot \eta_1^0 \cdot \eta_2^1) + \mathcal{O}(\epsilon^2 \cdot \eta_1^1 \cdot \eta_2^1) + \cdots + \mathcal{O}(\epsilon^2 \cdot \eta_1^i \cdot \eta_2^j). \end{aligned} \tag{13}$$

Only the first term in Equation (13) is retained, since it is the dominant one, to give the elastic energy per unit length:

$$\mathcal{E} = \varepsilon^{\mathrm{T}} \overline{S} \varepsilon, \tag{14}$$

where $\varepsilon^{\mathrm{T}} = [u_1' \;\; \theta' \;\; -u_3'' \;\; u_2'']$, which is the classical linear strain measures vector.

The matrix $\overline{S}$, which has a closed form solution given in Hodges and Volovoi (2000, 2002), is the 4×4 asymptotically-correct stiffness matrix, which is beyond the Euler–Bernoulli Theory of bending and St. Venant's Theory of torsion in terms of its rigor. It takes into account all in-plane warping deformations since γ_{12} is never assumed to be zero throughout the development, in addition to the shell bending strain measure ρ_{22}. Given the natural boundary conditions on the tip of the anisotropic thin-wall beam, the correct elastic response can be obtained from the flexibility matrix, which is the inverse of the stiffness matrix:

$$\varepsilon = \overline{S}^{-1} \left[\begin{array}{c} F_1 \\ M_{\theta'} \\ M_2 \\ M_3 \end{array}\right]. \tag{15}$$

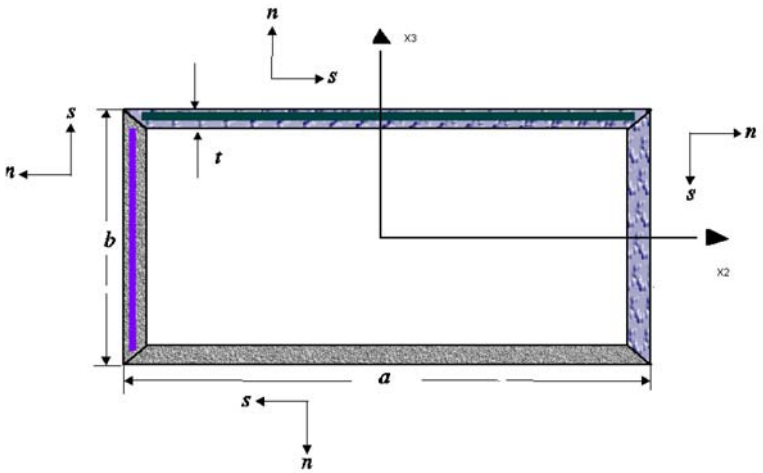

Fig. 2. Anisotropic single-cell box beam (Yu, 2005).

Table 1. The elements of the stiffness matrix obtained using the thin-walled anisotropic beam theory and VABS for Figure 2.

Stiffness Element	Thin-Walled	VABS (Popescu and Hodges, 2000)	Difference
S_{11}	1.2185×10^6 lb	1.2500×10^6 lb	2.52%
S_{12}	0.0522×10^6 lb − in	0.0521×10^6 lb − in	0.19%
S_{13}	0 lb − in	0 lb − in	Exact
S_{14}	0 lb − in	0 lb − in	Exact
S_{22}	0.1730×10^5 lb − in^2	0.1770×10^5 lb − in^2	2.26%
S_{23}	0 lb − in^2	0 lb − in^2	Exact
S_{24}	0 lb − in^2	0 lb − in^2	Exact
S_{33}	0.0508×10^6 lb − in^2	0.0543×10^6 lb − in^2	6.44%
S_{34}	0 lb − in^2	0 lb − in^2	Exact
S_{44}	0.1283×10^6 lb − in^2	0.1340×10^6 lb − in^2	4.25%

Implementation

Validation

The theory has been implemented in a MATLAB software module and validated against VABS. The first validation case was for a single-cell composite box beam VABS example shown in Figure 2.

The elements of the 4×4 stiffness matrix, $\overline{S}$, obtained from the implementation are compared to those produced by VABS in Table 1. Not all elements are shown since the stiffness matrix is symmetric.

The three-cell isotropic box beam shown in Figure 3 is another validation of the current implementation against VABS, where the stiffness matrix is now calculated about the lower-left corner of cross-section.

Similarly, The elements of the 4×4 stiffness matrix, $\overline{S}$, obtained from the implementation are compared to those produced by VABS in Table 2.

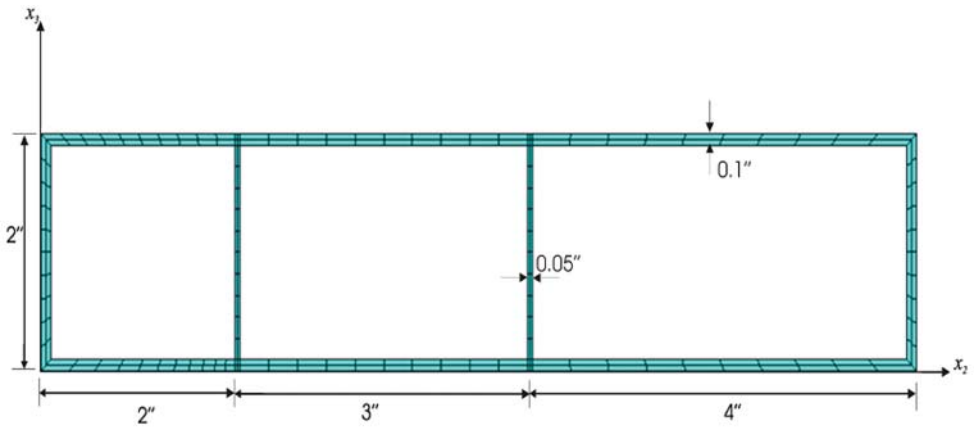

Fig. 3. Isotropic three-cells box beam (Yu, 2005).

Table 2. The elements of the stiffness matrix obtained using the thin-walled anisotropic beam theory and VABS for Figure 2.

Stiffness Element	Thin-Walled	VABS (Yu, 2005)	Difference
S_{11}	0.0611×10^{13} lb	0.0608×10^{13} lb	0.49%
S_{12}	0 lb − in	0 lb − in	Exact
S_{13}	0.0611×10^{13} lb − in	0.0608×10^{13} lb − in	0.49%
S_{14}	-0.2699×10^{13} lb − in	-0.2692×10^{13} lb − in	0.26%
S_{22}	0.0515×10^{13} lb − in^2	0.0540×10^{13} lb − in^2	4.63%
S_{23}	0 lb − in^2	0 lb − in^2	Exact
S_{24}	0 lb − in^2	0 lb − in^2	Exact
S_{33}	0.1073×10^{13} lb − in^2	0.1069×10^{13} lb − in^2	0.37%
S_{34}	-0.2699×10^{13} lb − in^2	-0.2692×10^{13} lb − in^2	0.26%
S_{44}	1.7091×10^{13} lb − in^2	1.7072×10^{13} lb − in^2	0.11%

The results presented in Tables 1 and 2 clearly validate the present implementation to model single/multi-cell thin-walled anisotropic cross-sections of rotor blades found on actual helicopters and turbine engines.

Applications

A two-cell anisotropic rotor blade with a SIKORSKY DBLN-526 Airfoil cross-section is the first example and it is depicted in Figure 4. Differences in the laminate design are highlighted by different line formats in Figure 4 including the webs, and they are given in Tables 3–5.

The solid-line region has elastic modula values that are the same as those in Table 3 but the wall thickness is 0.03 in, and the laminate stacking sequence is $[(40°/-40°/(30°/0°)_2)]$.

The stiffness matrix of this cross-section about the origin of the axes in Figure 4 was found to be:

$$\overline{S} = \begin{bmatrix} 0.4334 \times 10^{12} \text{ lb} & 0.9970 \times 10^{7} \text{ lb} - \text{in} & 0.3120 \times 10^{12} \text{ lb} - \text{in} & -0.1725 \times 10^{12} \text{ lb} - \text{in} \\ 0.9970 \times 10^{7} & 0.1094 \times 10^{9} \text{ lb} - \text{in}^2 & 0.7177 \times 10^{7} \text{ lb} - \text{in}^2 & -0.4463 \times 10^{8} \text{ lb} - \text{in}^2 \\ 0.3120 \times 10^{12} & 0.7177 \times 10^{7} & 1.2372 \times 10^{12} \text{ lb} - \text{in}^2 & -0.1792 \times 10^{10} \text{ lb} - \text{in}^2 \\ -0.1725 \times 10^{12} & -0.4463 \times 10^{8} & -0.1792 \times 10^{10} & 1.3014 \times 10^{12} \text{ lb} - \text{in}^2 \end{bmatrix}.$$

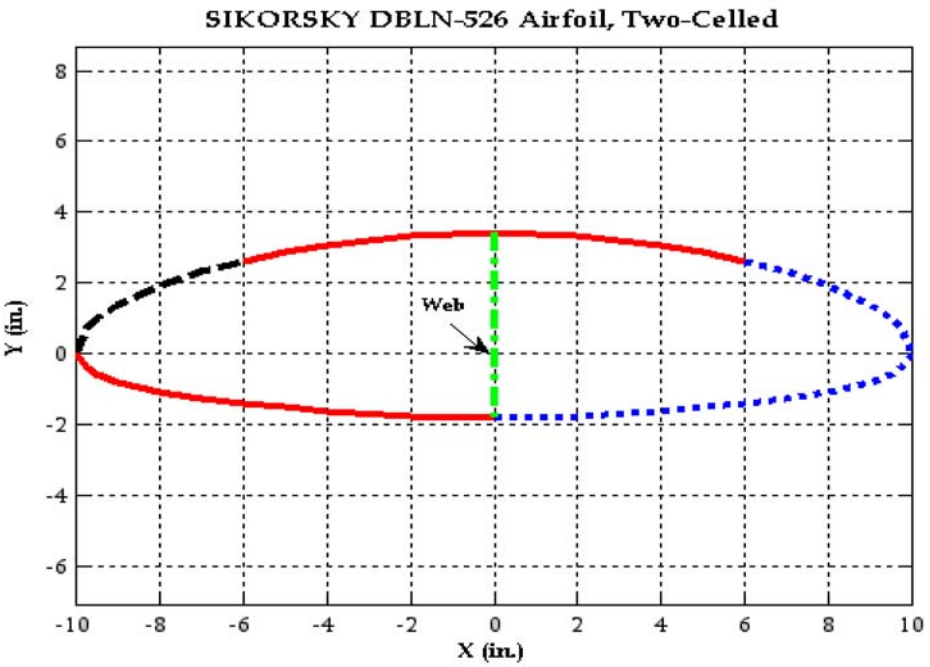

Fig. 4. Two-cell anisotropic SIKORSKY DBLN-526 Airfoil cross-section.

Table 3. Laminate design: dashed-line region in Figure 4.

Parameter	Value
wall thickness 'h'	0.01 in
laminate design	$[(0°/90°)]$, ply thickness = 0.005 in
E_l	20.59×10^6 psi
E_t	1.42×10^6 psi
G_{lt}	8.7×10^5 psi
G_{tn}	6.96×10^5 psi
$\nu_{lt} = \nu_{tn}$	0.42

Table 4. Laminate design: dotted-line region in Fig 4.

Parameter	Value
wall thickness 'h'	0.03 in
laminate design	$[45°/60°/-45°/0°/60°/45°]$, ply thickness = 0.005 in
E_l	0.11×10^{12} psi
E_t	0.02×10^{12} psi
G_{lt}	0.27×10^{11} psi
G_{tn}	0.96×10^{11} psi
ν_{lt}	0.37
ν_{tn}	0.42

Table 5. Laminate design: web region in Figure 4.

Parameter	Value
wall thickness 'h'	0.3 in
laminate design	[60°], ply thickness = 0.3 in
E_l	0.26×10^{12} psi
E_t	0.26×10^{12} psi
G_{lt}	0.1×10^{11} psi
G_{tn}	0.96×10^{11} psi
$\nu_{lt} = \nu_{tn}$	0.3

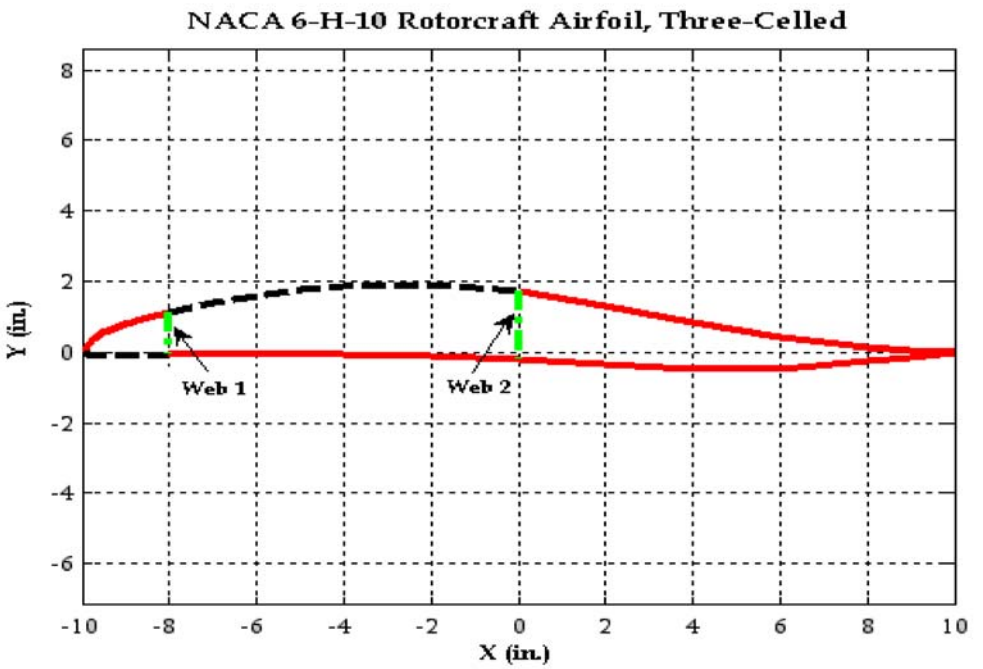

Fig. 5. Three-cells anisotropic NACA 6-H-10 Airfoil cross-section.

A second application example is the three-cells rotor blade cross-section shown in Figure 5.

The laminate design convention is the same as that for the previous example. The only exception is the second web, which has its ply fibre orientation at $-60°$ instead of $60°$ as in the first web. Similarly, the stiffness matrix of this cross-section about the origin of the axes in Figure 5 was found to be:

$$\overline{S} = \begin{bmatrix} 0.4018 \times 10^{11}\ \text{lb} & 0.7104 \times 10^{6}\ \text{lb}-\text{in} & 0.2683 \times 10^{11}\ \text{lb}-\text{in} & 1.2344 \times 10^{11}\ \text{lb}-\text{in} \\ 0.7104 \times 10^{6} & 0.2818 \times 10^{7}\ \text{lb}-\text{in}^2 & 0.1652 \times 10^{6}\ \text{lb}-\text{in}^2 & -0.4188 \times 10^{7}\ \text{lb}-\text{in}^2 \\ 0.2683 \times 10^{11} & 0.1652 \times 10^{6} & 0.2769 \times 10^{11}\ \text{lb}-\text{in}^2 & 0.6500 \times 10^{11}\ \text{lb}-\text{in}^2 \\ 1.2344 \times 10^{11} & -0.4188 \times 10^{7} & 0.6500 \times 10^{11} & 9.8795 \times 10^{11}\ \text{lb}-\text{in}^2 \end{bmatrix}.$$

Advantages

One must enumerate the advantages of this implementation in light of the fact that it will be utilized in tackling the dynamics of rotating blades for various research efforts in the Applied Dynamics Group at Carleton University. Relative to other specialized cross-sectional finite element packages like VABS and ABAQUS, the thin-walled asymptotic theory offers the following advantages:

- It provides a vast design space for parametric studies and easily interfaces with other disciplines like dynamics and control, which may necessitate keeping the information about the elastic deformation in a maximally compressed, yet correct, form.
- The meshing step and preparation of special input files are not required. The only input information required is the geometry of the airfoil (contour of the cross-section), which is readily available for any airfoil in simple and compact format, as well as the laminate design.
- As the thinness ratio increases, the analytical method becomes superior to VABS from the numerical point of view, since the finite element method results become unstable for high aspect ratio elements.
- It allows all but the essential variables to be eliminated offering a simple output and almost instantaneous execution time compared to more specialized software packages.

Conclusion

An implementation of a compact, yet comprehensive, asymptotically-correct anisotropic thin-wall theory to calculate the cross-sectional elastic constants of slender beams with airfoil-like cross-sections has been presented. It represents an essential step in the research efforts in the Applied Dynamics Group at Carleton University to model the structural dynamics of active rotor systems in maritime applications.

References

Badir, A.M. (1992). *Analysis of advanced thin-walled composite structures*. Ph.D., Georgia Institute of Technology.

Berdichevsky, V. (1982). On the energy of an elastic rod. *PMM*, 45, 518–529.

Berdichevsky, V., Armanios, E., and Badir, A. (1992). Theory of anisotropic thin-walled closed-cross-section beams. *Composites Engineering*, 2, 411–432.

Cesnik, C. and Hodges, D. (1997). VABS: A new concept for composite rotor blade cross-sectional modeling. *Journal of the American Helicopter Society*, 42(1), 27–38.

Cesnik, C. and Shin, S. (1998). Structural analysis for designing rotor blades with integral actuators. In *Proc. 39th AIAA Conf. on Structures, Structural Dynamics and Materials*, No. 2107, Long Beach, CA, AIAA.

Cesnik, C. and Shin, S. (2001a). On the modeling of integrally actuated helicopter blades. *International Journal of Solids and Structures*, 38, 1765–1789.

Cesnik, C. and Shin, S. (2001b). On the twist performance of a multiple-cell active helicopter blade. *Smart Materials and Structures*, 10, 53–61.

Cesnik, C., Sutyrin, V., and Hodges, D. (1993). A refined composite beam theory based on the variational-asymptotic method. In *Proceedings of the 34th Structures, Structural Dynamics, and Materials Conference*, No. 93-1616, La Jolla, CA, AIAA, pp. 2710–2720.

Cesnik, C.E.S. (1994). *Cross-sectional analysis of initially twisted and curved composite beams*. Ph.D., Georgia Institute of Technology.

Danielson, D. and Hodges, D. (1987). Nonlinear beam kinematics by decomposition of the rotation tensor. *Journal of Applied Mechanics*, 54, 258–262.

Hodges, D. and Patil, M. (2005). Correlation of geometrically-exact beam theory with the princeton data. *Journal of the American Helicopter Society*, 49(3), 357–360.

Hodges, D. and Volovoi, V. (2000). Theory of anisotropic thin-walled beams. *Journal of Applied Mechanics*, 67, 453–459.

Hodges, D. and Volovoi, V. (2002). Single- and multi-celled composite thin-walled beams. *AIAA Journal*, 40(5), 960–965.

Popescu, B. and Hodges, D. H. (2000). On asymptotically correct timoshenko-like anisotropic beam theory. *International Journal of Solids and Structures*, 37:535–558.

Volovoi, V., Hodges, D., Cesnik, C., and Popescu, B. (2001). Assessment of beam modeling methods for rotor blade application. *Mathematical and Computer Modelling*, 33, 1099–1112.

Yu, W. (2005). *VABS Manual and Examples*. Georgia Institute of Technology, Utah State University.

Yu, W., Volovoi, V., Hodges, D., and Hong, X. (2002). Validation of the variational asymptotic beam sectional analysis (VABS). *AIAA Journal*, 40(10), 2105–2113.